Thompson, A. R., & Davie, E. W. (1971) *Biochim. Biophys. Acta 250*, 210.
Uhteg, L. C., & Lundblad, R. L. (1974) *Fed. Proc., Fed. Am. Soc. Exp. Biol. 33*, 1388.
van Nispen, J. W., Hageman, T. C., & Scheraga, H. A. (1977) *Arch. Biochem. Biophys. 182*, 227.
Von Dreele, P. H., Rae, I. D., & Scheraga, H. A. (1978) *Biochemistry 17*, 956.
Wider, G., Macura, S., Kumar, A., Ernst, R. R., & Wüthrich, K. (1984) *J. Magn. Reson. 56*, 207.
Winzor, D. J., & Scheraga, H. A. (1964) *Arch. Biochem. Biophys. 104*, 202.

High-Resolution NMR Studies of Fibrinogen-like Peptides in Solution: Structure of a Thrombin-Bound Peptide Corresponding to Residues 7–16 of the Aα Chain of Human Fibrinogen†

Feng Ni, Yvonne C. Meinwald, Max Vásquez,‡ and Harold A. Scheraga*
Baker Laboratory of Chemistry, Cornell University, Ithaca, New York 14853-1301
Received July 7, 1988; Revised Manuscript Received October 11, 1988

ABSTRACT: The interaction of the following human fibrinogen-like peptides with bovine thrombin was studied by one- and two-dimensional NMR techniques in aqueous solution: acetyl-Phe(8)-Leu(9)-Ala(10)-Glu(11)-Gly(12)-Gly(13)-Gly(14)-Val(15)-Arg(16)-Gly(17)-Pro(18)-NHMe (F6), acetyl-Phe-Leu-Ala-Glu-Gly-Gly-Gly-Val-Arg(16) (tF6), acetyl-Asp(7)-Phe-Leu-Ala-Glu-Gly-Gly-Gly-Val-Arg(16)-Gly(17)-Pro-Arg(19)-Val(20)-NHMe (F8), and acetyl-Asp-Phe-Leu-Ala-Glu-Gly-Gly-Gly-Val-Arg(16) (tF8). At pH 5.3 and 25 °C, the Arg(16)–Gly(17) peptide bonds in both F6 and F8 were cleaved instantaneously in the presence of 0.5 mM thrombin, producing truncated peptides tF6 and tF8 and other peptide fragments. On the basis of observations of line broadening, thrombin was found to bind to the cleavage products, tF6 and tF8, of peptides F6 and F8. Peptide tF8 may have a higher affinity for thrombin than peptide tF6, as suggested by the more pronounced thrombin-induced line broadening on the proton resonances in peptide tF8. Transferred NOE (TRNOE) measurements were made of the complexes between thrombin and peptides tF6 and tF8. Medium- and long-range NOE interactions were found between the NH proton of Asp(7) and the $C^{\beta}H$ protons of Ala(10), between the $C^{\alpha}H$ proton of Glu(11) and the NH proton of Gly(13), and between the ring protons of Phe(8) and the $C^{\alpha}H$ protons of Gly(14) and the $C^{\gamma}H$ protons of Val(15). Sets of structures of the decapeptide tF8 were deduced by use of distance geometry calculations based on sequential and medium- and long-range TRNOEs from the thrombin-bound peptide. A predominant feature of these structures is the nonpolar cluster formed by the side chains of residues Phe(8), Leu(9), and Val(15) that are directly involved in binding to thrombin. This structural feature is brought about by an α-helical segment involving residues Phe(8)–Ala(10), followed by a multiple-turn structure involving residues Glu(11)–Val(15). These results provide an explanation for the observations that Asp(7), Phe(8), and Gly(12) are strongly conserved in mammalian fibrinogens and that the mutations of Asp(7) to Asn(7) and of Gly(12) to Val(12) result in delayed release of fibrinopeptide A, producing human bleeding disorders.

In this series of papers, we have examined the interactions between thrombin and the N-terminal portion (residues 1–23) of the Aα chain of human fibrinogen. In the accompanying paper (Ni et al., 1989), we reported NMR[1] evidence for the direct involvement of residues Asp(7), Phe(8), Leu(9), Val(15), and Arg(16) of human fibrinogen-like peptides in a complex with bovine thrombin. We also discussed transferred NOE measurements that revealed there is a chain reversal within residues Asp(7)–Arg(16), so that a distant residue, Phe(8), is brought close to Val(15) near the peptide bond between Arg(16) and Gly(17) that is cleaved by thrombin. However, the detailed backbone structure of residues Asp(7)–Arg(16) could not be further defined because of peak overlaps with resonances from residues Ala(1)–Gly(6). In this paper, we present transferred NOE studies of the interaction of bovine thrombin with synthetic peptides corresponding to residues Phe(8)–Pro(18) (F6; Meinwald et al., 1980; Marsh et al., 1982, 1985) and to residues Asp(7)–Val(20) (F8; Marsh et al., 1983). Sets of structures of the thrombin-bound decapeptide corresponding to residues Asp(7)–Arg(16) were derived by use of distance geometry calculations based on the

† This work was supported by research grants from the National Institute of General Medical Sciences (GM-24893) and the National Heart, Lung and Blood Institute (HL-30616) of the National Institutes of Health. It was carried out with the GN-500 500-MHz NMR spectrometer at the NIH Regional Research Resource for Multinuclear NMR and Data Processing located at Syracuse University (RR-01317). This is paper 18 in a series. Ni et al. (1989) is paper 17 of this series.
* Author to whom correspondence should be addressed.
‡ Present address: Tripos Associates Inc., St. Louis, MO 63144.

[1] Abbreviations: NMR, nuclear magnetic resonance; NOE, nuclear Overhauser effect; TRNOE, transferred NOE; NOESY, two-dimensional nuclear Overhauser and exchange spectroscopy; COSY, two-dimensional scalar correlation spectroscopy; DQ-COSY, double-quantum filtered COSY; EDTA, ethylenediaminetetraacetic acid; ECEPP, empirical conformational energy program for peptides; FpA, fibrinopeptide A; HPLC, high-performance liquid chromatography.

0006-2960/89/0428-3094$01.50/0

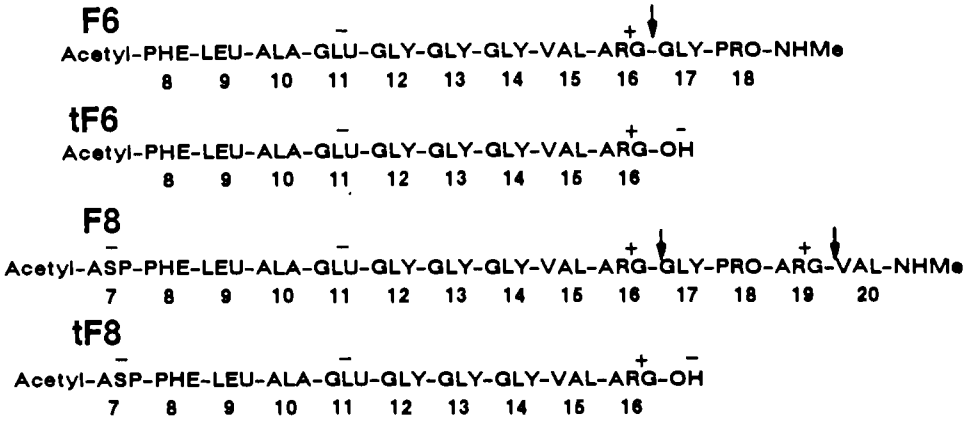

FIGURE 1: Amino acid sequences of the peptides used in the study. The numbering is that of the Aα chain of human fibrinogen, and the charges are those at neutral pH. The arrows in each sequence indicate the peptide bonds cleaved by thrombin.

transferred NOE measurements.

Experimental Procedures

Preparation and Purification of Peptides and Bovine Thrombin. The peptides, F6 and F8, were those synthesized and described previously (Meinwald et al., 1980; Marsh et al., 1982, 1983, 1985). Further purification of the peptide material was achieved by use of a reverse-phase HPLC procedure reported in our earlier paper (Ni et al., 1988). The peaks from the eluted peptide material were symmetric in shape, suggesting that the synthesized material is homogeneous. The purified peptides were further characterized by amino acid analyses, which were performed with a Waters Pico Tag amino acid analysis system at the Cornell University Biotechnology Program Facility. The samples were hydrolyzed and derivatized according to the method of Bidlingmeyer et al. (1984). The amino acid composition of F6 was Glu (0.93, 1), Gly (4.13, 4), Arg (1.03, 1), Ala (0.91, 1), Pro (1.05, 1), Val (0.98, 1), Leu (0.99, 1), Phe (0.99, 1). That of peptide F8 was Asp (1.00, 1), Glu (1.05, 1), Gly (4.05, 4), Arg (2.24, 2), Ala (0.99, 1), Pro (1.03, 1), Val (1.70, 2), Leu (0.98, 1), Phe (0.98, 1).

Bovine thrombin was prepared by use of the procedure of Ghosh and Seegers (1980) and purified as described by Ni et al. (1989).

NMR Sample Preparation and Measurements. Stock solutions of the peptides, F6 and F8, were prepared by dissolving appropriate amounts of the peptides in 0.4 mL of H_2O and 0.1 mL of an aqueous solution that was 150 mM in NaCl, 50 mM in sodium phosphate, and 0.1 mM in EDTA. The pH values of the resulting peptide solutions were then adjusted to 5.3 by use of trace amounts of 1 M HCl or 1 M NaOH. The pH-adjusted solutions were freeze-dried to increase the peptide concentration. The dried powders (including salt and peptides) were taken up in a mixture of 60 μL of H_2O and 40 μL of D_2O so that the concentrations of the peptides were all about 25 mM. The pH values of the aqueous samples were all checked with an Ingold electrode without correction for the presence of D_2O. NMR samples of the peptide-thrombin solutions were prepared by mixing 0.3 mL of the thrombin stock solution and 0.1 mL of the peptide solutions prepared above. The concentrations of thrombin in the NMR samples were determined before and after the NMR experiments by its absorbance, using the value of $E^{280}_{1\%} = 19.5$ (Winzor & Scheraga, 1964). The concentrations of the peptides were calibrated against standards by quantitative determination of peak areas in the HPLC chromatograms of the peptides in fixed volumes of the NMR samples.

NMR experiments were carried out as described in the accompanying paper (Ni et al., 1989). Two-dimensional transferred NOE measurements were carried out with a weak decoupling irradiation at the water proton frequency during a postacquisition delay of 1.5 s for a more complete recovery of the *z*-magnetization and for more efficient solvent suppression.

Results

Resonance Assignments. The NH proton resonances of both F6 and F8 (Figure 1) have been partially assigned (Marsh et al., 1985). Other resonances were assigned in aqueous solution at pH 5.3 by use of the NMR techniques discussed in our previous paper (Ni et al., 1988). Briefly, the spin patterns were assigned to specific residues by an analysis of the phase-sensitive DQ-COSY spectra of the peptides in D_2O (Wüthrich, 1986). Sequence-specific assignments were then made by the combined analysis of phase-sensitive NOESY and DQ-COSY spectra of the peptides at 5 °C, pH 5.3, in H_2O solutions (Wüthrich, 1986). The chemical shifts of all proton resonances of various residues in F8 are similar to those in F10 under similar solvent conditions (Ni et al., 1988). In F6, the NH proton resonances of Phe(8), Leu(9), Ala(10), Glu(11), and Gly(12) are shifted downfield by 0.08, 0.09, 0.06, 0.04, and 0.02 ppm, respectively. All other protons appear essentially at the same chemical shifts as the corresponding protons in F8 or F10 (Ni et al., 1988).

The assignment of the resonances in peptides tF6 and tF8 is illustrated in Figure 2, where the transferred $C^{\alpha}H$–NH NOEs (see later section) of the thrombin–tF8 complex are displayed with the sequential NOE connectivities indicated. The pattern is very similar to that of the same sequence found in natural FpA [residues Ala(1)–Arg(16) of the Aα chain of human fibrinogen] (Ni et al., 1988). This pattern remains the same even after the enzyme–peptide complexes are kept in an ice bath for over a 2-month period. This indicates that no other cleavages by thrombin occurred in the peptide and that the system is very stable for NMR experiments.

Interaction of Thrombin with Peptides F6 and F8. Thrombin interacts with peptides F6 and F8 in a similar manner as with peptide F10 studied in the preceding paper (Ni et al., 1989). The Arg(16)–Gly(17) peptide bonds were cleaved within the first few minutes after the peptides were mixed with thrombin (at a concentration of 0.5 mM). The N-terminal cleavage products, tF6 and tF8, remain bound to thrombin, as indicated by the line broadening of the backbone NH and aromatic proton resonances of the peptides, tF6 and tF8, in the presence of 0.1 equiv (compared to the peptides) of thrombin (Figure 3). Similarly, some of the side-chain proton resonances are also broadened upon binding to thrombin, compared to those of Val(20) in F8 which is cleaved off

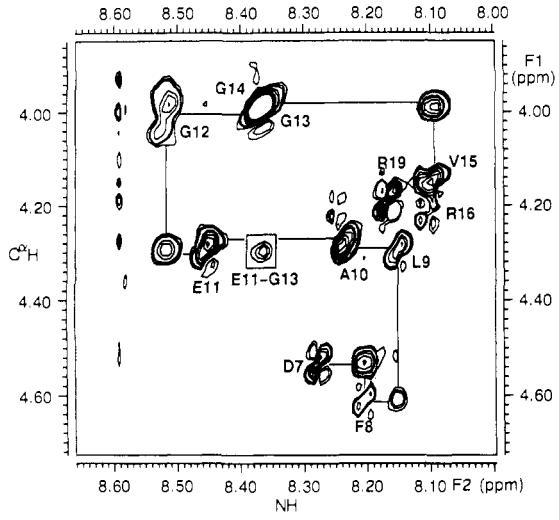

FIGURE 2: Sequential $C^{\alpha}H$–NH TRNOE connectivities of peptide tF8. Every intraresidue NH–$C^{\alpha}H$ cross peak is labeled by the corresponding amino acid residues involved (Figure 1). The boxed cross peak has been assigned to the NOE interaction between the $C^{\alpha}H$ proton of Glu(11) and the NH proton of Gly(13). The spectrum was acquired at 15 °C, pH 5.3, with a mixing time of 200 ms (see also Figure 5). The concentration of thrombin was 0.5 mM, and that of the peptide was 6 mM.

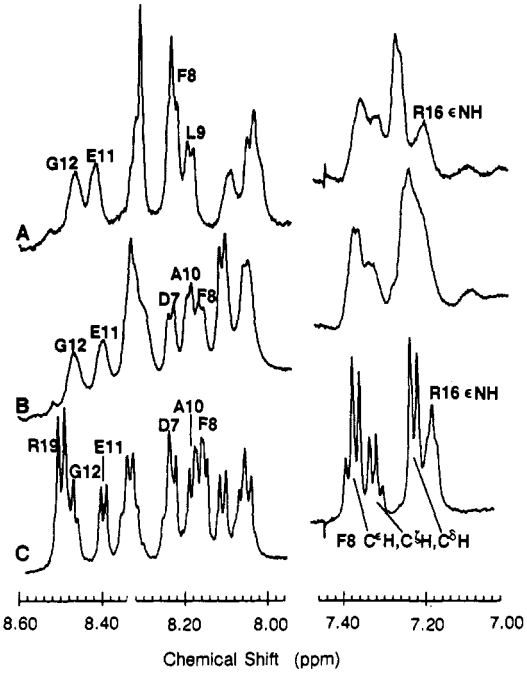

FIGURE 3: Resonances of the NH and ring protons of Phe(8) in peptides F6 (A) and F8 (B) in the presence of thrombin, and in peptide F8 in the absence of thrombin (C) in *buffered* H_2O solution at pH 5.3 and 25 °C. Peptide concentrations were 6 mM, and the concentration of thrombin was 0.5 mM. On the left, some of the peaks in the NH region are labeled by the corresponding amino acid residues (Figure 1). On the right are the aromatic regions of the same spectra.

by thrombin (Figure 4). The NH proton resonances of Glu(11) and Gly(12) in peptides tF6 (Figure 3A) and tF8 (Figure 3B), for example, are strongly affected by the presence of thrombin compared to those in the isolated peptide F8 (Figure 3C). Again, the most pronounced effect is on the aromatic protons of Phe(8) (Figure 3). Other broadened resonances are those of the $C^{\beta}H$ protons of Asp(7), Phe(8), Ala(10), and Arg(16), the $C^{\delta}H$ protons of Leu(9), and the $C^{\gamma}H$ protons of Val(15) [cf. Figure 4 of this paper with Figure 7 of Ni et al. (1989)].

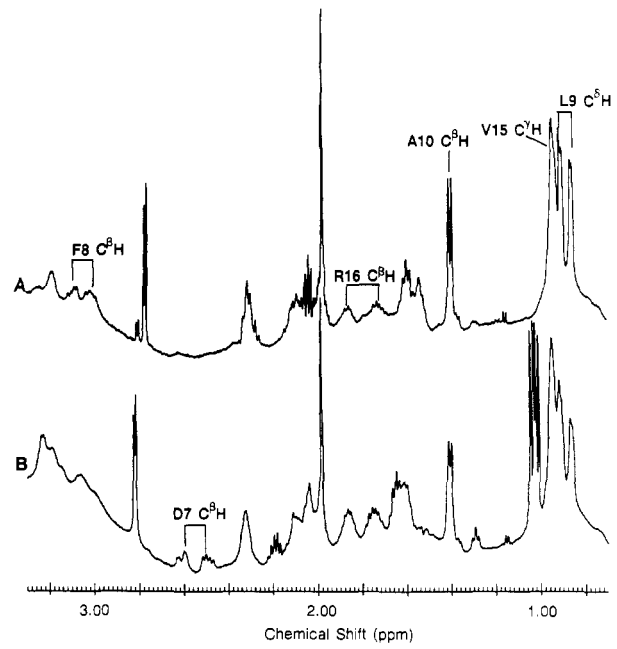

FIGURE 4: Thrombin-induced resonance line broadening in mixtures of thrombin with peptides F6 (A) and F8 (B) in *buffered* H_2O solution at pH 5.3 and 25 °C. The concentration of thrombin was 0.5 mM in both cases; the concentrations of F6 and F8 were both 6 mM. Some of the resonances are labeled by the residues involved. The multiplet at 1.04 ppm in (B) corresponds to the $C^{\gamma}H$ proton resonances of Val(20), which is cleaved off by thrombin. The difference in resolution and peak heights of the doublet of the resonance of the $C^{\beta}H$ protons of Ala(10) in both tF6 (A) and tF8 (B) should be noted. In a separate experiment (see text), this difference was found to be due to the possibly higher binding affinity of peptide tF8 (compared to tF6) toward thrombin.

In Figure 4, we see that the resonances of the $C^{\beta}H$ protons of Ala(10) in peptide tF8 (Figure 4B) seem to be more affected by thrombin than those in peptide tF6 (Figure 4A). These differences might be due to slight differences in the concentrations of thrombin and the peptides in the NMR sample; we therefore prepared a series of samples (five for each peptide) of peptides F6 and F8, with a final concentration of F6 equal to 1.0 ± 0.1 mM and that of F8, 1.4 ± 0.1 mM, as determined by quantitative amino acid analysis. These samples also contained different volumes of thrombin (from the same preparation) with the final concentrations of thrombin varied from 48 to 140 μM. In the limit of fast exchange, the observed line broadening on the proton resonances of peptides by enzyme binding increases with a decrease of the ratio of the concentrations of the peptide and the enzyme [Gerig & Reinheimer, 1970; Dwek, 1973; Figure 7 of Ni et al. (1989)]. Since the ratio of tF8 to thrombin (10:1 to 29:1) is larger than that of tF6 to thrombin (7:1 to 21:1), we would expect that proton resonances in peptide tF6 would be more broadened than those in peptide tF8 at the same concentration of thrombin. However, an analysis of the one-dimensional proton spectra of these samples (not shown) revealed that the extent of line broadening of the resonances of the $C^{\beta}H$ protons of Ala(10) in peptide tF8 (1.4 ± 0.1 mM) in the presence of 48 μM of thrombin could be brought about only by a higher concentration (140 μM) of thrombin with peptide tF6 (1.0 ± 0.1 mM). The less pronounced line broadening in peptide tF6 may be interpreted as a result of the lower binding affinity of tF6 (compared to tF8) toward thrombin, since it has been shown that peptide F8 is a much better substrate for thrombin (Marsh et al., 1983).

Transferred NOEs of Thrombin-Bound Peptides. At 500 MHz, neither peptide tF6 nor tF8 exhibits NOEs in aqueous

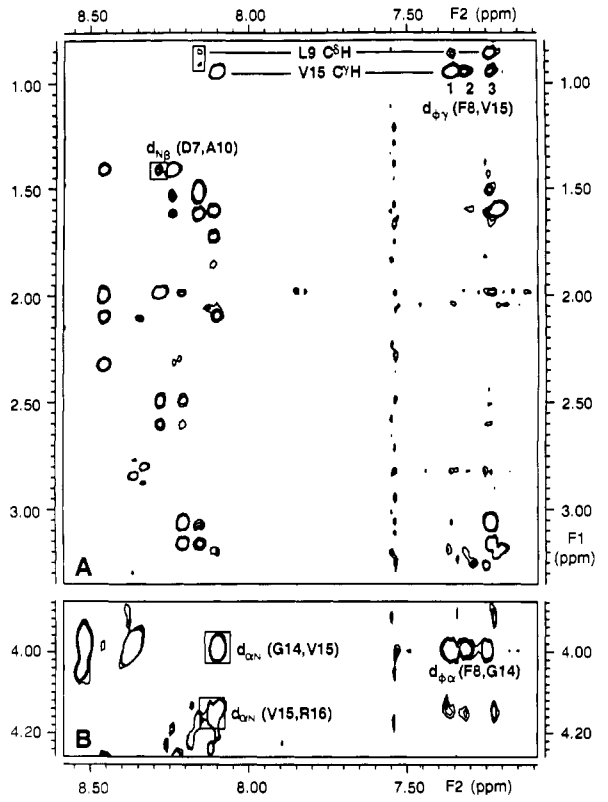

FIGURE 5: Selected regions of the transferred NOE spectrum of the complex of thrombin with peptide tF8 at pH 5.3. The NOESY spectrum was acquired (see also Figure 2) with a mixing time of 200 ms at 15 °C. Thrombin concentration was 0.5 mM; peptide concentration was 6 mM. (A) NOEs between the NH and aromatic resonances (F2 axis) and the C$^{\beta}$H and other aliphatic proton resonances (F1 axis). (B) NOEs between the NH and aromatic resonances (F2 axis) and a selected region of the C$^{\alpha}$H proton resonances (F1 axis). The medium-range NOEs between Asp(7) and Ala(10) and the long-range NOEs between Phe(8) and Gly(14) and Val(15) are indicated by the protons involved. The positions of peaks 1, 2, and 3 on the F2 frequency axis correspond to the meta (ϵ), para (ζ), and ortho (δ) protons, respectively, of the aromatic ring of Phe(8) (see also Figure 3). The *absence* of the cross peak between the C$^{\delta}$H protons of Leu(9) and the para (ζ) proton of Phe(8) should be noted.

solution at 25 °C; however, NOEs are observed when either peptide forms a complex with thrombin. The reason for this behavior is discussed in the accompanying paper (Ni et al., 1989).

Transferred NOEs have been observed in the interaction of thrombin with fibrinogen-like peptides in the preceding paper (Ni et al., 1989). In previous sections, we discussed the use of transferred NOEs for the sequence-specific resonance assignments of the thrombin cleavage products, tF6 and tF8, of peptides F6 and F8 (Figure 2). In further analysis, the intensities of NOE cross peaks were classified into three categories: strong, medium, and weak. Strong NOEs correspond to very intense cross peaks in the spectra obtained at different mixing times (50–200 ms) and temperatures (5–25 °C) or to cross peaks that prevail under all conditions such as the C$^{\alpha}$H–NH interaction between Glu(11) and Gly(12) (Figure 2). Cross peaks observed only at longer mixing times (200 ms) and at lower temperatures (15 °C) are treated as very low intensity (weak) NOEs. Other cross peaks were classified as medium NOEs.

To distinguish possible NOE cross peaks from thrombin itself, the experiment was repeated at various temperatures, since the resonance peaks from the peptides shift in a known manner (Marsh et al., 1985; Ni et al., 1988). Furthermore, possible NOE cross peaks from thrombin were located by a

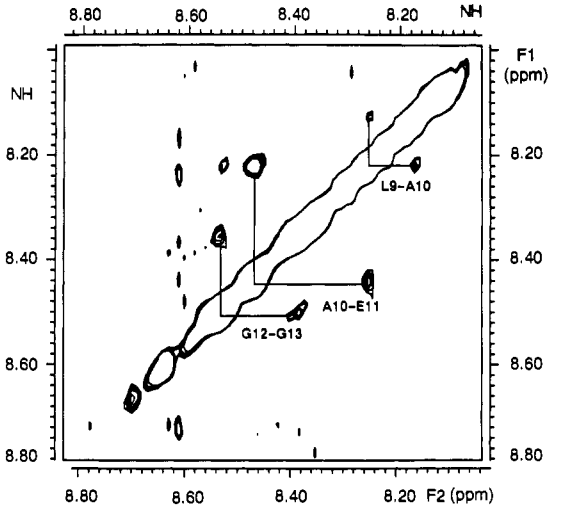

FIGURE 6: NH–NH region of the TRNOE spectrum (acquired as described in Figure 5) of the complex of thrombin with peptide tF8 at pH 5.3. The NOEs are labeled by the amino acid residues involved.

combined analysis of the TRNOE spectra of the complex of thrombin with different fibrinogen-like peptides (Ni et al., 1989).

In Figure 5, we present two regions of the two-dimensional TRNOE spectra of the complex of peptide tF8 with thrombin obtained at 15 °C and a mixing time of 200 ms. Under these conditions, the TRNOE effects are still highly selective: there are cross peaks between the C$^{\delta}$H protons belonging to *one* methyl group of Leu(9) and the ortho or meta ring protons of Phe(8), but no NOE can be seen between the same methyl protons of Leu(9) and the para ring protons of Phe(8) (Figure 5A). In addition to similar NOEs in the complex of thrombin with fibrinopeptide A (see Table I in the preceding paper), sequential C$^{\beta}$H–NH NOEs were also observed between residues Asp(7) and Phe(8), between Phe(8) and Leu(9), and between Leu(9) and Ala(10) (Figure 5A). There are also strong NH–C$^{\beta}$H and weak NH–C$^{\gamma}$H intraresidue interactions in Arg(16) (Figure 5A) and strong sequential C$^{\alpha}$H–NH interactions between residues Val(15) and Arg(16) of peptide tF8 (Figures 2 and 5B). The existence of these extra TRNOEs in tF8 is due to a more complete magnetization recovery in transferred NOE measurements with a longer postacquisition delay of 1.5 s (see Experimental Procedures), compared to 800 ms used in the preceding paper (Ni et al., 1989). These missing sequential TRNOEs from the interaction of thrombin with fibrinopeptide A were indeed recovered in further transferred NOE experiments with longer postacquisition delays (1.5 s; spectra not shown). It is interesting that sequential TRNOEs were still not observed, in these new TRNOE experiments, between the C$^{\beta}$H protons of Glu(11) and the NH proton of Gly(12), between the NH protons of Glu(11) and Gly(12), between the NH protons of Gly(14) and Val(15), and between the C$^{\beta}$H proton of Val(15) and the NH proton of Arg(16). These NOEs were also not observed in the interaction of thrombin with peptides tF8 (Figures 5A and 6) and in the complex of thrombin with tF6 (spectra not shown). More importantly, however, is the observation of an i–(i + 2) interaction between the C$^{\alpha}$H proton of Glu(11) and the NH proton of Gly(13), as indicated in Figure 2. A similar peak is also present in the TRNOE map of the thrombin–tF6 complex (spectrum not shown). This NOE was not found in the interaction of FpA with thrombin because the NH protons of Glu(5) and Gly(13) overlap with each other (Ni et al., 1988), and this peak is masked by the strong antiphase multiplet peaks from the zero-quantum coherence transfers

between the $C^{\alpha}H$ and NH protons of Glu(5) (Ni et al., 1989).

Long-range NOEs were also found in the thrombin–tF8 complex (and in the thrombin–tF6 complex, spectrum not shown) between all ring protons of Phe(8) and the $C^{\gamma}H$ protons of Val(15) (Figure 5A) and between all ring protons of Phe(8) and the $C^{\alpha}H$ protons of Gly(13) or Gly(14) (their $C^{\alpha}H$ protons are not resolved) (Figure 5B). In the preceding paper, the Phe(8)–Gly interaction was temporarily assigned to that arising from Phe(8) and Gly(14) in the complex of thrombin with fibrinopeptide A (Ni et al., 1989). This ambiguity of the interactions between Phe(8) and Gly(13) or Gly(14) has now been resolved by studying the interaction of thrombin with peptide F6 where the $C^{\alpha}H$ protons of Gly(13) had been selectively replaced by deuterons during synthesis [D_2-Gly-(13)–F6; Marsh et al., 1985]. It was found that the NOEs between Phe(8) and Gly persist in the complex of thrombin with D_2-Gly(13)–tF6, indicating that they arise from the interactions of Phe(8) with Gly(14) instead of Gly(13).

There is a weak cross peak between the NH proton of Asp(7) and the $C^{\beta}H$ protons of Ala(10) (Figure 5A). A similar cross peak has also been found between Asp(7) and Ala(10) in the complex of thrombin with another peptide with a Cys residue preceding Asp(7) [in the latter peptide, the NH proton resonance of Asp(7) is shifted; unpublished results]. This cross peak has thus been assigned to the medium-range NOE interaction between Asp(7) and Ala(10).

In the free state, only very weak NH–NH NOEs were observed for F6 and F8 even when the temperature was lowered to −8 °C (spectra not shown). In the presence of thrombin, there are strong sequential NH–NH NOEs between Gly(12) and Gly(13) and between Ala(10) and Glu(11) in the thrombin–tF8 complex at 15 °C (Figure 6). These same NH–NH NOEs were also found in the interaction of thrombin with peptide tF6. The existence of these two NH–NH NOEs demonstrates that thrombin interacts with peptides tF6 and tF8 in a similar manner and similarly with FpA (Ni et al., 1989). Furthermore, because of a slight resonance shift caused by the absence of residues Ala(1)–Gly(6), the NH resonances of Leu(9) and Ala(10) in tF8 (with the N-terminus blocked by the acetyl group; see Figure 1) are resolved from each other, revealing an NH–NH NOE between these two residues (Figure 6).

Peptide Backbone Structure and NOE Distance Constraints. In the thrombin–peptide complex, the binding region from Asp(7) to Arg(16) presumably adopts a unique conformation. Thrombin-induced NOEs (TRNOEs) thus provide a set of interproton distances of less than 5 Å, which are indicative of the structure of the thrombin-bound peptide. In the thrombin-bound state of peptide tF8, Asp(7) is close to Ala-(10), as indicated by the TRNOE between the NH proton of Asp(7) and the $C^{\beta}H$ protons of Ala(10) (Figure 5A). The aromatic side chain of Phe(8) is folded into proximity with residues Gly(14) and Val(15) since there exist TRNOEs between the ring protons of Phe(8) and the $C^{\alpha}H$ protons of Gly(14) and the $C^{\gamma}H$ protons of Val(15) (Figure 5). Furthermore, there is a tight hydrophobic cluster formed by the nonpolar side chains of residues Phe(8), Leu(9), and Val(15). This nonpolar cluster is identified on the basis of the TRNOEs between protons on the side chains of the involved residues (Figure 5A).

The overall structural features discussed above for the bound peptide may be brought about by specific backbone conformations of residues Asp(7)–Val(15). In contrast to the type I′ β-turn identified for the *isolated* peptide (Ni et al., 1988), there is a chain reversal involving residues Glu(11) and Gly-(12) of the *bound* peptide, suggested by a TRNOE between the $C^{\alpha}H$ proton of Glu(11) and the NH proton of Gly(13) (Figure 2). This chain reversal involves either a half-turn or a type II β-turn on the basis of the presence of *strong* NOEs between the $C^{\alpha}H$ proton of Glu(11) and the NH proton of Gly(12) and between the NH protons of Gly(12) and Gly(13) (Wagner et al., 1986; Wüthrich, 1986). The existence of either type of turn is also compatible with the *absence* of TRNOEs between the NH protons of Glu(11) and Gly(12) and between the $C^{\beta}H$ protons of Glu(11) and the NH proton of Gly(12) discussed in the previous section. Other local backbone conformations can also be identified by the intensity characteristics of sequential $C^{\alpha}H$–NH and NH–NH NOEs (Leach et al., 1977; Billiter et al., 1982; Wüthrich et al., 1984; Wagner et al., 1986; Wüthrich, 1986). An additional β-turn (type II′) in the bound peptide, involving residues Gly(14) and Val(15), is suggested by the presence of *strong* $C^{\alpha}H$–NH NOEs between Gly(14) and Val(15) and between Val(15) and Arg(16) and by the *absence* of an NH–NH NOE between the NH protons of Gly(14) and Val(15). Unfortunately, a possibly weak NOE between the $C^{\alpha}H$ proton of Gly(14) and the NH proton of Arg(16), as one would expect if a type II′ β-turn exists between residues Gly(14) and Val(15) (Wüthrich et al., 1984), could not be identified due to the partial overlap of the NH proton resonance of Val(15) with that of Arg(16) (Figure 2). The two strong NH–NH NOEs between Leu(9) and Ala(10) and between Ala(10) and Glu(11) are indicative of α-helical conformations for Leu(9) and Ala(10) (Wagner et al., 1986). These backbone conformations are further supported by the existence of only *weak* NOEs between the $C^{\alpha}H$ proton of Leu(9) and the NH proton Ala(10) and between the $C^{\alpha}H$ proton of Ala(10) and the NH proton of Glu(11) (Wagner et al., 1986).

To proceed with a more precise determination of the structure of the thrombin-bound peptide, it is necessary to convert the NOE and other structural information such as slow NH exchange of some residues (Ni et al., 1988) into distance information. Accurate interproton distances can be obtained from the nuclear cross-relaxation rates (Solomon, 1955), which, in turn, can be measured by use of the initial buildup rates of the intensities of the NOE cross peaks between dipolar coupled protons (Macura & Ernst, 1980). Since all residues within the region Asp(7)–Arg(16) in fibrinopeptide A are directly involved in the interaction with thrombin (Ni et al., 1989), peptide tF8 should inherit the correlation time of the thrombin–peptide complex during the period of time when the NOE interaction is occurring (transferred NOEs). In the current study, it is difficult to assess the relative flexibility of different parts of peptide tF8 (or tF6) in the thrombin-bound state. We therefore assume a uniform correlation time for all NOE interactions observed for the bound peptides. Under such an assumption, an unknown distance r_{ij} can be calculated from a known distance r_{kl} by using

$$r_{ij} = r_{kl}(\sigma_{kl}/\sigma_{ij})^{1/6} \quad (1)$$

where σ_{ij} and σ_{kl} are the cross relaxation rates between protons i and j and between protons k and l, respectively. However, we did not attempt to calculate *exact* distances from an internal standard according to the above equation because of the low signal-to-noise character of the transferred NOEs and because of the uncertainty in the dynamic properties of different parts of the bound peptide. We estimated only upper bounds and some lower bounds of interproton distances (Table I) by calibration against known distances such as that (2.5 Å) between the $C^{\delta}H$ and the $C^{\epsilon}H$ protons on the aromatic ring

Table I: Distance Constraints Derived from the TRNOE and NH Exchange Experiments

Sequential with Lower Bounds Set to 3.5 Å		
Hz Phe(8)	HD Leu(9)	
HB Glu(11)	HN Gly(12)	
HN Glu(11)	HN Gly(12)	
HN Gly(14)	HN Val(15)	
HB Val(15)	HN Arg(16)	
Intraresidue with Upper Bounds Set to 2.5 Å		
HN to HB, HB to HD	Phe(8)	
HN to HB	Leu(9)	
HN to HB	Ala(10)	
HN to HB, HA to HB	Glu(11)	
HN to HG	Val(15)	
HN to HB, HB to HE	Arg(16)	
Intraresidue with Upper Bounds Set to 3.0 Å		
HN to HB	Asp(7)	
HA to HD	Phe(8)	
HA to HG, HN to HG	Glu(11)	
HN to HB	Val(15)	
Intraresidue with Upper Bounds Set to 4.0 Å		
HN to HD	Leu(9)	
HN to HD	Arg(16)	
Sequential with Upper Bounds Set to 2.5 Å		
HA Asp(7)	HN Phe(8)	
HB Phe(8)	HN Leu(9)	
HA Glu(11)	HN Gly(12)	
HA Gly(14)	HN Val(15)	
Sequential with Upper Bounds Set to 3.0 Å		
HB Asp(7)	HN Phe(8)	
HD Phe(8)	HB Leu(9)	
HD Phe(8)	HD Leu(9)	
HB Leu(9)	HN Ala(10)	
HN Leu(9)	HN Ala(10)	
HB Ala(10)	HN Glu(11)	
HN Ala(10)	HN Glu(11)	
HN Gly(12)	HN Gly(13)	
HA Val(15)	HN Arg(16)	
Sequential with Upper Bounds Set to 3.5 Å		
HA Phe(8)	HN Leu(9)	
HE Phe(8)	HD Leu(9)	
HA Leu(9)	HN Ala(10)	
HA Ala(10)	HN Glu(11)	
Medium-Range Upper Bounds		
HN Asp(7)	HB Ala(10)	3.5 Å
HA Glu(11)	HN Gly(13)	3.5 Å
O Ala(10)	HN Gly(13) (H-bond)	2.2 Å
O Glu(11)	HN Gly(14) (H-bond)	2.2 Å
O Gly(13)	HN Arg(16) (H-bond)	2.2 Å
Long-Range Upper Bounds		
HD Phe(8)	HA Gly(14)	3.5 Å
HE Phe(8)	HA Gly(14)	3.0 Å
HZ Phe(8)	HA Gly(14)	3.5 Å
HE Phe(8)	HG Val(15)	3.0 Å
HD Phe(8)	HG Val(15)	3.5 Å
HZ Phe(8)	HG Val(15)	3.5 Å

of residue Phe(8), using a procedure similar to that described elsewhere (Williamson et al., 1985). In brief, intensities of all the rest of the NOE cross peaks at different mixing times are compared to the intensities of the cross peak between these ring protons. At shorter mixing times (50 or 100 ms), it was difficult to measure the intensities of the NOE cross peaks between the aromatic ring protons since they are too close to the diagonal. As discussed in the previous section, we have identified a half-turn or a type II β-turn involving residues Glu(11) and Gly(12). The distance between the $C^{\alpha}H$ proton of Glu(11) and the NH proton of Gly(12) was calibrated to have an upper bound of 2.5 Å, which was used as a secondary standard, especially at short mixing times. Thus, if, at a mixing time of 50 ms, the TRNOE cross peak between any two protons is as strong as that between the $C^{\alpha}H$ proton of Glu(11) and the NH proton of Gly(12), the distance of that interacting proton pair was assigned an upper bound of 2.5 Å. These strong NOEs arise, e.g., from interactions between the $C^{\alpha}H$ proton of Asp(7) and the NH proton of Phe(8) and between the $C^{\alpha}H$ protons of Gly(14) and the NH proton of Val(15) (Figure 2). The distances of proton pairs with weak NOE cross peaks at 50-ms mixing time or with *intense* cross peaks at 100-ms mixing time were assigned upper bounds of 3.0 Å. These include, e.g., the sequential interaction between one of the $C^{\beta}H$ protons of Asp(7) and the NH proton of Phe(8) and the long-range interactions between the $C^{\epsilon}H$ protons of Phe(8) and the $C^{\gamma}H$ protons of Val(15). An upper bound of 3.5 Å was assigned to the distances between proton pairs with *weak* NOEs at a mixing time of 100 ms, such as those between the $C^{\epsilon}H$ protons of Phe(8) and the $C^{\delta}H$ protons belonging to one of the methyl groups of Leu(9), between the $C^{\zeta}H$ proton of Phe(8) and the $C^{\gamma}H$ protons of Val(15), and between the NH proton of Asp(7) and the $C^{\beta}H$ protons of Ala(10). Protons with barely observable NOEs at 200-ms mixing time were assumed to be separated by less than 4.0 Å. This category includes the interaction between the NH proton and the $C^{\delta}H$ protons of Leu(9) (Figure 5A). The intraresidue and sequential interresidue distances thus obtained were further checked for consistency by comparison with distance upper bounds calibrated against NOEs of the aromatic ring protons obtained with a mixing time of 200 ms. These distances were consistent with the distribution of the sequential proton distances of the peptide chain (Leach et al., 1977; Billiter et al., 1982). In fact, the distance estimates may represent pessimistic values since an upper bound of 3.0 Å between the NH and the $C^{\beta}H$ protons of Val(15) would allow the ϕ dihedral angle to fall in the region of positive ϕ in the ϕ–ψ map (Leach et al., 1977), whereas it is known that a Val residue cannot assume stable backbone conformations with positive ϕ dihedral angles (Zimmerman et al., 1977; Némethy & Scheraga, 1977; Richardson, 1981; Iijima et al., 1987).

For proton pairs with observable NOE, lower bounds of their distances were limited by the van der Waals contacts, which are incorporated as part of the distance geometry program (Vásquez & Scheraga, 1988). As discussed in the previous section, all *sequential* NOEs were observed between resolved protons in the thrombin-bound peptide except for those between the $C^{\beta}H$ protons of Glu(11) and the NH proton of Gly(12), between the NH protons of Glu(11) and Gly(12), between the NH protons of Gly(14) and Val(15), and between the $C^{\beta}H$ protons of Val(15) and the NH proton of Arg(16). Since other NOEs involving those protons were observed, larger distances must be the cause for the absence of these sequential NOEs in the interaction of thrombin with all fibrinogen-like peptides with mixing times from 50 to 200 ms at all temperatures from 5 to 25 °C. To utilize the NOE information fully, lower bounds of 3.5 Å were assumed for those proton pairs with missing *sequential* TRNOEs. Incorporation of these lower bounds should help define the local β-turn structure involving residues Glu(11) and Gly(12) and residues Gly(14) and Val(15). The *only* other lower bound involving missing nonsequential TRNOEs is for the distance (<3.5 Å) between the $C^{\zeta}H$ proton of Phe(8) and $C^{\delta}H$ protons belonging to one of the methyl groups of Leu(9) (Figure 5A). This lower bound should restrict the relative orientation of the aromatic ring of Phe(8) with respect to the side chain of Leu(9) since TRNOEs were clearly seen between the methyl group of Leu(9) and all other ring protons of Phe(8) (Figure 5A). In other studies, utilization of the absence of NOEs has

also been found to result in better defined structures that satisfy observed NOE information (Fesik et al., 1987; Olejniczak et al., 1988).

In the accompanying paper, it was proposed, on the basis of the observation of the distribution of sequential NOEs, that thrombin selectively binds to one particular conformation from an ensemble of conformational states in the *isolated* peptide F10 [residues Ala(1)–Arg(23)] (Ni et al., 1989). A type II′ β-turn involving residues Gly(14) and Val(15) of the thrombin-bound peptide accounts for the reduced NH exchange rate of Arg(16) observed for the isolated peptide F10 (Ni et al., 1988). A type II β-turn involving residues Glu(11) and Gly(12) in the thrombin-bound peptide requires that the NH proton of Gly(13) be hydrogen bonded to the carbonyl oxygen of Ala(10) (Rose et al., 1985). The NH proton of Gly(13) was indeed also observed to have a reduced exchange rate in both peptides F6 and F8 (Marsh et al., 1985).[2] Furthermore, the NH protons of Gly(13) and Gly(14) may both exchange slowly since their NH resonances are not sufficiently resolved from each other (Ni et al., 1988). In addition, both Gly(13) and Gly(14) possess abnormal temperature coefficients of the NH chemical shifts in peptides F6, F8, F11 (FpA), and F10 (Marsh et al., 1985; Ni et al., 1988), indicating that their NH protons are either involved in hydrogen bonds or are shielded from the solvent. Model building (incorporating the long-range NOEs discussed in the previous sections) indicates that the NH proton of Gly(14) may be hydrogen bonded to the carbonyl oxygen of Glu(11). Distance constraints from these hydrogen bonds (Table I) have also been incorporated in some of the distance geometry calculations discussed below.

Distance Geometry Calculations and Molecular Modeling. An implementation of a variable-target-function procedure (Braun & Gō, 1985) was used for the generation of sets of terminally blocked decapeptide (*N*-acetyl-Asp-Phe-Leu-Ala-Glu-Gly-Gly-Gly-Val-Arg-NHMe) conformations that were free of steric overlaps and that were consistent with the NMR information. This information consisted of upper and lower bounds of inter- and intraresidue proton–proton distances derived from the TRNOE and NH exchange experiments (Table I). The details of the computational procedure have been reported elsewhere (Vásquez & Scheraga, 1988). There were, however, some major differences between the procedure used here and that used previously.

For groups of protons with overlapping resonances, a weighted sum of individual distances was forced to satisfy the upper bound. In other words, if a given NOE is due to the interaction of n_1 equivalent or indistinguishable protons (e.g., the three methyl protons of an alanine residue) with n_2 other equivalent protons, this would introduce a term in the target function of the form

$$F = [(\sum_{k=1}^{n_1}\sum_{l=1}^{n_2} r_{kl}^{-6})^{-1/6} - \mathrm{upp}]_+^2 \qquad (2)$$

where upp is the upper bound deduced from the observation of the given NOE, r_{kl} is the calculated distance between protons k and l (where it is understood that the indices k and l refer to the lists of n_1 and n_2 equivalent protons, respectively), and the notation $[\,]_+$ means that the term inside the bracket is taken as equal to zero unless the term is strictly positive; viz., if this term is negative, it means that the modified distance is smaller than the upper bound upp, and therefore it should not contribute to the penalty function. This expression reduces to the usual (Braun & Gō, 1985) functional form when both n_1 and n_2 are equal to 1. A similar treatment has been used in previous work (Clore et al., 1986; Fesik et al., 1987; Olejniczak et al., 1988), and its results in a more efficient utilization of the information stored in the short-range (intraresidue and sequential) NOE peaks and in overall better defined structures.

In the complex of tF8 with thrombin, one of the critical long-range TRNOE peaks involves ortho (δ) [or meta (ε)] protons in the aromatic ring of Phe(8) interacting with the $C^{\gamma}H$ protons of Val(15) (Table I). The interpretation based on the usual corrections (Wüthrich et al., 1983; Wüthrich, 1986) leads to a modification of these critical interactions resulting in an extra 4.3 Å on the upper bounds. That is, approximately 2.15 Å comes from the C^{γ} (or C^{ζ}) to H^{δ} (or H^{ϵ}) standard distance (Momany et al., 1975) in aromatic rings, plus an approximately equivalent, 2.15 Å, distance between the $C^{\gamma}H$ protons and the β carbon of Val(15). These are the most conservative corrections that have to be introduced if the upper bound is now to be defined between the γ (or ζ) carbon of the Phe(8) residue and the β carbon of Val(15). This is a worst-case interpretation of the data, which may lead to a loosely defined polypeptide structure. Therefore, this procedure was replaced by use of eq 2.

To improve the efficiency of the computation, a contact energy of 20 instead of 5 kcal/mol was first used to define steric overlaps (increasing the value of the contact energy is equivalent to assigning a lower weight to the steric contact penalty term of the object function being optimized). In other words, for a given pair of atoms, a steric overlap was penalized if the interatomic distance was smaller than that giving rise to a value of 20 kcal/mol for the respective nonbonded term of the ECEPP (Momany et al., 1975) interaction energy of the atomic pair. With this assignment of contact energy, distance constraints were incorporated sequentially (Braun & Gō, 1985), starting from 100 conformations randomly sampled from the single-residue-based backbone dihedral angle distributions (Zimmerman et al., 1977; Vásquez & Scheraga, 1988). Structures with values of the distance part of the objective function smaller than 1.0 were then selected, and these were subjected to a second optimization, using a contact energy of 10 instead of 20 kcal/mol and incorporating all the distance constraints at once (in contrast to the sequential incorporation used above). This same procedure was repeated, using a contact energy of 5 kcal/mol and, finally, a contact energy of 3 kcal/mol to define steric overlaps.

The above computations were first carried out by using sets of distance constraints derived from the TRNOE *alone* (Table I). Structures thus generated were checked for the satisfaction of distance constraints by use of two criteria: a structure should have a maximum distance violation of less than 0.5 Å, *and* all other violations should be less than 0.3 Å. A total of 12 structures were found with an average deviation of 2.2 Å among them, when all heavy backbone atoms of residues from

[2] In the work of Marsh et al. (1985), the exchange rate of an NH proton in peptides F6 and F8 was found to be smaller than that in other shorter fibrinogen-like peptides. This NH proton was assigned to Gly(14) on the basis of an analysis of the NH region of the one-dimensional proton spectra of a peptide corresponding to residues Gly(12)–Pro(18) and with specific deuterations at the $C^{\alpha}H$ protons of Gly(13) (Marsh et al., 1985). However, reinspection of Figure 3 in Marsh et al. (1985) revealed that this same resonance should be assigned to the NH proton of Gly(13) instead of that of Gly(14). This new assignment is confirmed by an inspection of the NH region of the proton spectra of peptide tF6 [with specific deuterations at the $C^{\alpha}H$ protons of Gly(13)] complexed to thrombin (Figure 3A)]. In fact, the appearance of a *singlet* instead of a doublet of doublets at about 8.32 ppm indicates that this resonance is decoupled (by deuteration) from the coupling of the NH and $C^{\alpha}H$ protons. Therefore, the positions of the NH protons of Gly(13) and Gly(14) reported in our previous paper (Figure 2; Ni et al., 1988) should be interchanged, as indicated in Figure 2 in the present paper.

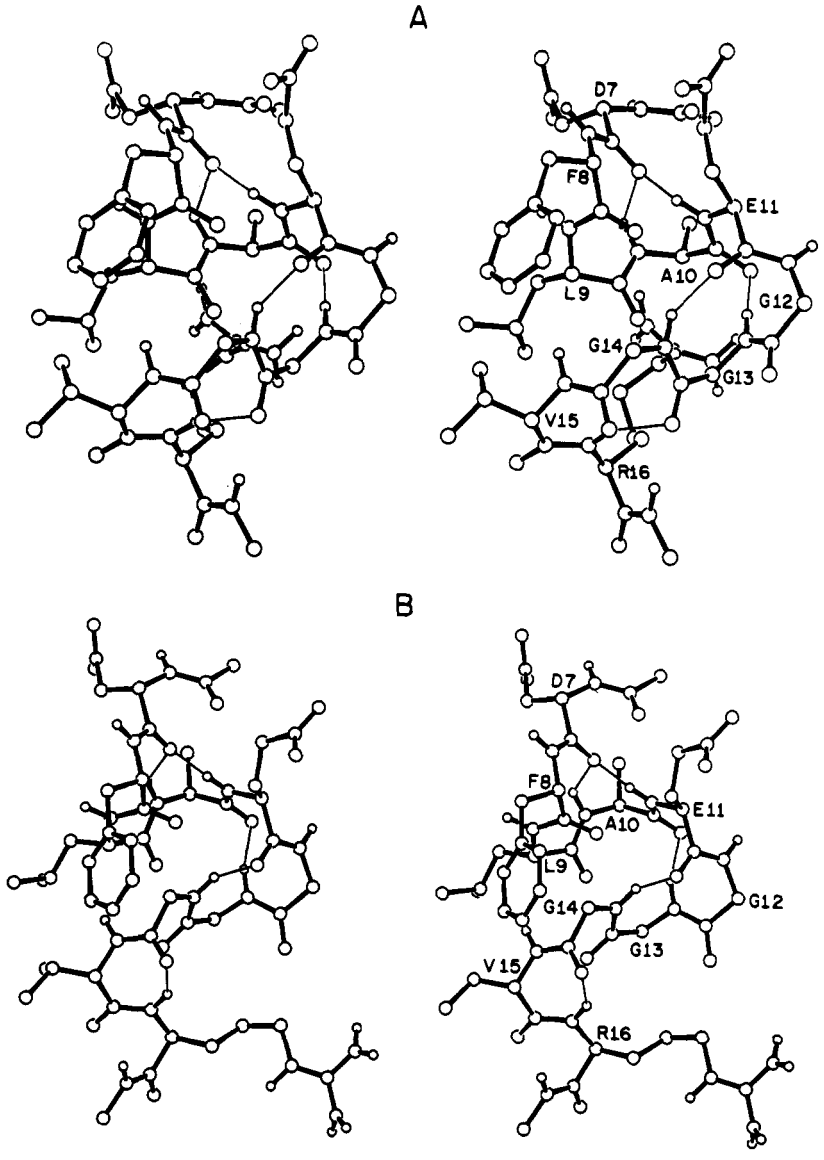

FIGURE 7: Proposed structure (stereo drawings) of the thrombin-bound tF8 (A) without imposing any hydrogen-bond constraints (structure I in Table II) and (B) with imposition of the hydrogen-bond constraints in the distance geometry calculations. In both structures, a thin line connecting an oxygen atom to a hydrogen atom indicates that those two atoms are separated by less than 2.0 Å (hydrogen bonds). The C^{α} atoms are labeled by the corresponding amino acid residues (Figure 1). In both (A) and (B), the nonpolar cluster formed by the side chains of Phe(8), Leu(9), and Val(15) is clearly seen. Since there were no TRNOE constraints on the relative orientation of the Arg side chain, it adopted two different conformations in the two calculated structures shown here.

Asp(7) to Val(15) were considered [Table II; Arg(16) was left out in the evaluation of the RMS deviation since some of the TRNOE information pertaining to this residue is ambiguous because of resonance overlappings]. The chain segment from Asp(7) to Gly(12) is better defined, as indicated by an average deviation of 1.7 Å for the backbone atoms of these residues among the 12 converged structures. In the TRNOE-based structures, the carbonyl oxygen of Asp(7) is invariably hydrogen bonded to the NH proton of Glu(11), as illustrated in the stereo drawing (Figure 7A) of structure I in Table II. Residues Phe(8), Leu(9), and Ala(10) assume the α-helical backbone conformation in most of the 12 structures. Asp(7) and Glu(11) are both half-α-helical in that, as mentioned above, the carbonyl oxygen of Asp(7) and the NH proton of Glu(11) are involved in hydrogen bonding and the C^{α} atoms of both residues are both part of the short α-helix (Figure 7A), even though the backbone dihedral angles of these residues may not assume the values for α-helical conformations (Levitt & Greer, 1977; Kabsch & Sander, 1983). Furthermore, in most of these structures, Gly(12) is in the region of positive values of ϕ in the ϕ–ψ map, where only a Gly or an Ala residue can occur with high probability (Zimmerman et al., 1977; Némethy & Scheraga, 1977; Richardson, 1981; Iijima et al., 1987). More interestingly, β-turn conformations for residues Glu(11)–Val(15) are also generated by using TRNOE distance constraints alone, resulting in the hydrogen bonds discussed in the previous section (Table II and Figure 7A).

In the TRNOE-based structures, the region from Gly(13) to Val(15) is more poorly defined compared to residues Asp(7)–Gly(12), as indicated by a decrease of 0.5-Å RMS deviation if residues Gly(13), Gly(14), and Val(15) are not included in the RMS evaluation (Table II). The reason for this is that TRNOEs pertaining to residues Gly(13) and Gly(14) could not be assigned because of the resonance overlaps between the $C^{\alpha}H$ protons of Gly(12), Gly(13), and Gly(14) and between the NH protons of residues Gly(13) and Gly(14) (Figure 2). To define the backbone conformations of these residues better, distance geometry calculations were carried out by using both the TRNOE and the proposed hy-

Table II: Typical Backbone Conformations[a] and Values of RMS Deviations (RMSD) of the Backbone Atoms of the Computer-Optimized Structures of the Decapeptide

	7	8	9	10	11	12	13	14	15	16	RMSD (Å)
	Asp	Phe	Leu	Ala	Glu	Gly	Gly	Gly	Val	Arg	(Backbone)[b]
I	F	A	A	A	C	A*	A*	A	B	C	2.2 (1.7)
II	F	A	A	A	C	A*	A*	C*	B	A	1.8 (1.6)

[a] The one-letter codes for backbone conformations were defined in Zimmerman et al. (1977). Letter A, for example, refers to the α-helical region. A* refers to the region of left-handed α-helix. C and F refer to the regions of extended conformation. It should be noted that only Gly and Ala can adopt low-energy backbone conformations in the region of positive values of ϕ in the ϕ–ψ map. Structure I was among the 12 converged structures (2.2-Å RMS deviation) generated from the TRNOE distance constraints *alone* (Table I). Structure II, on the other hand, was one of the 17 converged structures (1.8-Å RMS deviation) based on the TRNOE distance constraints and the proposed hydrogen bonds (see text). [b] The values of RMS deviations correspond to averages of *all* pairwise comparisons between individual structures (Vâsquez & Scheraga, 1988). Arg(16) was not included in the computation of the RMS deviation since some of the TRNOE information of Arg(16) is ambiguous because of resonance overlappings. The values of RMS deviations in parentheses are those for the backbone atoms of residues Asp(7)–Gly(12) between the converged structures.

drogen-bond distance constraints listed in Table I. There are very small differences between the backbone conformations of residues Asp(7) and Gly(12) in this new set of structures (1.7-Å RMS deviation among the 17 structures) and those in the TRNOE-based structures (1.6-Å RMS deviation among the 12 structures) (Table II). Evidently, the overall differences between the 17 converged structures are smaller in the new set, as indicated by a 1.8-Å RMS deviation of all backbone atoms of residues from Asp(7) to Val(15). In Figure 7B, we present the stereo drawing of structure II in Table II. It can be seen that the overall features of the structures in Figure 7 are very similar. Included in Table III are the atomic coordinates for the structure in Figure 7A, which may serve as a basis for the design of thrombin-specific inhibitors.

Discussion

In the preceding paper, it was established that residues Asp(7)–Arg(16) of the Aα chain of human fibrinogen constitute an essential structural element in its interaction with thrombin (Ni et al., 1989). It was found here that the N-terminally-blocked peptide tF8 indeed binds to thrombin in a manner similar to that of FpA, as indicated by the similarity of the thrombin-induced line broadening (Figures 3B and 4B) and the distributions of transferred NOEs (Table I). The more pronounced line broadening on some side-chain proton resonances in peptide tF8 (Figure 4) may be caused by the higher affinity of tF8 (compared to tF6) toward thrombin, since it has been shown that peptide F8 is a much better substrate for thrombin than peptide F6 (Marsh et al., 1983) and residues Gly(17)–Arg(19) did not contribute significantly to the interaction (Ni et al., 1989). Asp(7) in itself, therefore, assumes a special importance in the specificity of the interaction of thrombin with fibrinogen. In the sets of structures generated by distance geometry calculations, the carbonyl oxygen of Asp(7) is invariably hydrogen bonded to the NH proton of Glu(11) (Figure 7), in agreement with the observation (Ni et al., 1988) that the exchange rate of the NH proton of Glu(11) is reduced compared to that of Glu(5) within FpA. Furthermore, a simple rotation of the side chain of Asp(7) places the side-chain carboxylate group within hydrogen-bonding distances to the NH protons of Phe(8), Leu(9), or Ala(10) (Figure 7). The interaction of the carboxylate oxygens with these NH protons would account for the reduced NH exchange rates of Phe(8), Leu(9), and Ala(10) reported previously for peptide F10 (Ni et al., 1988). The pH titration of the amide proton resonances in peptide F13 [residues Ala(1)–Val(20)] has also provided direct evidence for a weak hydrogen bond between the carboxylate oxygen of Asp(7) and the NH proton of Leu(9) at both 25 and −8 °C (Ni et al., 1989). Furthermore, the deletion of Asp(7) results in downfield shifts of 0.08, 0.09, and 0.06 ppm of the NH proton resonances of residues Phe(8), Leu(9), and Ala(10), respectively, in the free peptide, an observation favoring the existence of the aforementioned hydrogen bond between Asp(7) and Leu(9). Side-chain–backbone hydrogen bonds involving non-α-helical conformations of Asp have been found previously by energy-minimization calculations on terminally blocked single residues (Lewis et al., 1973). The presence of Asp(7) thus brings significant stabilizing interactions by means of hydrogen bonds within the peptide (both free and bound). These results provide an explanation for the observations that Asp(7) is strongly conserved in many species with replacements only by Glu (Blombäck, 1967; Henschen et al., 1983). On the other hand, it has been reported that the mutation of Asp(7) to Asn(7) results in delayed release of fibrinopeptide A and produces bleeding disorders (Henschen et al., 1983; Ménaché, 1983, and references cited therein), although it has recently been reported that Asn can also stabilize α-helical segments in residues in proteins that follow Asp or Asn (Presta & Rose, 1988; Richardson & Richardson, 1988). Therefore, the negative charge of the carboxylate group of either an Asp(7) or a Glu(7) residue may also play an important role in the interaction of thrombin with fibrinogen.

In the preceding paper (Ni et al., 1989), we have discussed the importance of a hydrophobic cluster formed by the nonpolar side chains of Phe(8), Leu(9), and Val(15) in the interaction of thrombin with fibrinogen. In Figure 7, this hydrophobic cluster is on the left-hand side of the illustrated structures. From an inspection of the computer-generated structures, it was found that the diameter of this cluster is less than 8 Å, a value in agreement with the upper limit of the hydrophobic binding site near the active site of thrombin, proposed on the basis of spin-labeling studies (Berliner et al., 1981; Berliner, 1984). The nonpolar side chains of Phe(8), Leu(9), and Val(15) thus form the complementary hydrophobic combining site of the substrate when thrombin binds to fibrinogen. This conclusion is further supported by the observations that both Phe(8) and Val(15) are strongly conserved, and Leu(9) has been replaced only by Ile in many mammalian species (Blombäck, 1967; Henschen et al., 1983). Such hydrophobic interactions account for the requirement for Phe–Leu in maintaining catalytic efficiency of the thrombin cleavage of the Arg–Gly peptide bonds in synthetic fibrinogen-like peptides (van Nispen et al., 1977). It also explains why the placement of a Phe residue at position P3 [in place of Gly(14)] enhances the inhibitory effects of peptide methyl esters on thrombin action (Blombäck et al., 1969). In fact, it has been demonstrated by NMR measurements (Rae & Scheraga, 1979) that in a tripeptide with D-Phe, but not with L-Phe, at the P3 position the aromatic ring of the Phe residue is bent directly over the side chain of Val. The D-Phe peptide was found to be a much better substrate (Claeson et al., 1977), as would be predicted by this model.

A prominent feature in the structure of the thrombin-bound peptide is the α-helical conformations of residues Phe(8)–Ala(10), followed by multiple-turn backbone conformations of residues Glu(11)–Val(15) (Table II). Residues Gly(12)

Table III: Atomic Coordinates of the Structure of the Decapeptide (Acetyl-Asp-Phe-Leu-Ala-Glu-Gly-Gly-Gly-Val-Arg-NHMe) from Which the Structure in Figure 7A Was Constructed

atom	residue	sequence no.	x (Å)	y (Å)	z (Å)	atom	residue	sequence no.	x (Å)	y (Å)	z (Å)
1, H3	CH_3	1	−2.613	−1.974	0.244	76, HB	Glu^-	6	1.517	−6.439	0.980
2, H3	CH_3	1	−2.577	−0.419	−0.621	77, CG	Glu^-	6	1.139	−4.510	0.093
3, H3	CH_3	1	−2.336	−0.463	1.142	78, HG	Glu^-	6	0.058	−4.409	−0.003
4, C	CH_3	1	−2.151	−0.988	0.205	79, HG	Glu^-	6	1.539	−3.509	0.255
5, O	CO	1	−0.182	−2.249	−0.154	80, CD	Glu^-	6	1.719	−5.095	−1.196
6, C	CO	1	−0.682	−1.136	0.000	81, OE2	Glu^-	6	0.971	−5.113	−2.198
7, N	Asp^-	2	0.000	0.000	0.000	82, OE1	Glu^-	6	2.896	−5.511	−1.151
8, HN	Asp^-	2	−0.423	0.906	0.000	83, N	Gly	7	−0.318	−7.030	3.832
9, CA	Asp^-	2	1.453	0.000	0.000	84, HN	Gly	7	−1.192	−7.034	3.345
10, HA	Asp^-	2	1.739	−0.090	−1.048	85, CA	Gly	7	−0.207	−8.007	4.902
11, CB	Asp^-	2	2.004	1.294	0.602	86, HA	Gly	7	−1.199	−8.371	5.171
12, C	Asp^-	2	1.959	−1.169	0.848	87, HA	Gly	7	0.365	−8.867	4.556
13, O	Asp^-	2	1.240	−1.671	1.710	88, C	Gly	7	0.470	−7.398	6.132
14, HB	Asp^-	2	1.748	1.322	1.661	89, O	Gly	7	1.075	−8.113	6.930
15, HB	Asp^-	2	3.092	1.273	0.538	90, N	Gly	8	0.345	−6.084	6.247
16, CG	Asp^-	2	1.500	2.580	−0.057	91, HN	Gly	8	−0.149	−5.510	5.594
17, OD2	Asp^-	2	0.797	3.339	0.644	92, CA	Gly	8	0.937	−5.371	7.366
18, OD1	Asp^-	2	1.830	2.774	−1.247	93, HA	Gly	8	0.834	−4.297	7.212
19, N	Phe	3	3.192	−1.567	0.573	94, HA	Gly	8	0.399	−5.614	8.282
20, HN	Phe	3	3.770	−1.153	−0.130	95, C	Gly	8	2.415	−5.730	7.525
21, CA	Phe	3	3.802	−2.668	1.300	96, O	Gly	8	2.875	−6.007	8.632
22, HA	Phe	3	3.457	−3.592	0.837	97, N	Gly	9	3.119	−5.715	6.402
23, CB	Phe	3	5.318	−2.478	1.210	98, HN	Gly	9	2.737	−5.489	5.506
24, C	Phe	3	3.385	−2.651	2.772	99, CA	Gly	9	4.536	−6.036	6.403
25, O	Phe	3	2.823	−3.623	3.273	100, HA	Gly	9	4.668	−7.117	6.345
26, HB	Phe	3	5.695	−3.047	0.361	101, HA	Gly	9	5.009	−5.610	5.518
27, HB	Phe	3	5.531	−1.428	1.009	102, C	Gly	9	5.219	−5.500	7.662
28, CG	Phe	3	6.075	−2.905	2.469	103, O	Gly	9	5.409	−6.234	8.630
29, CD1	Phe	3	6.269	−4.226	2.730	104, N	Val	10	5.571	−4.223	7.608
30, CD2	Phe	3	6.553	−1.965	3.327	105, HN	Val	10	5.413	−3.633	6.816
31, HD1	Phe	3	5.886	−4.979	2.042	106, CA	Val	10	6.229	−3.580	8.732
32, CE1	Phe	3	6.972	−4.622	3.899	107, HA	Val	10	6.749	−4.354	9.296
33, CE2	Phe	3	7.255	−2.361	4.496	108, CB	Val	10	7.272	−2.581	8.227
34, HD2	Phe	3	6.397	−0.906	3.118	109, C	Val	10	5.174	−2.937	9.635
35, HE1	Phe	3	7.128	−5.681	4.108	110, O	Val	10	5.452	−1.951	10.316
36, CZ	Phe	3	7.450	−3.682	4.757	111, HB	Val	10	7.880	−3.084	7.474
37, HE2	Phe	3	7.639	−1.607	5.183	112, CG2	Val	10	8.199	−2.136	9.359
38, HZ	Phe	3	7.989	−3.986	5.654	113, CG1	Val	10	6.601	−1.377	7.562
39, N	Leu	4	3.676	−1.534	3.424	114, HG1	Val	10	5.848	−0.965	8.233
40, HN	Leu	4	4.134	−0.748	3.009	115, HG1	Val	10	7.351	−0.617	7.347
41, CA	Leu	4	3.338	−1.378	4.828	116, HG1	Val	10	6.127	−1.693	6.633
42, HA	Leu	4	4.055	−1.964	5.404	117, HG2	Val	10	8.525	−3.009	9.926
43, CB	Leu	4	3.498	0.082	5.258	118, HG2	Val	10	9.069	−1.630	8.940
44, C	Leu	4	1.938	−1.943	5.078	119, HG2	Val	10	7.665	−1.453	10.019
45, O	Leu	4	1.721	−2.665	6.049	120, N	Arg^+	11	3.986	−3.522	9.612
46, HB	Leu	4	4.147	0.582	4.540	121, HN	Arg^+	11	3.768	−4.324	9.056
47, HB	Leu	4	2.523	0.566	5.199	122, CA	Arg^+	11	2.888	−3.019	10.420
48, CG	Leu	4	4.065	0.309	6.661	123, HA	Arg^+	11	3.175	−1.998	10.675
49, HG	Leu	4	4.216	−0.663	7.131	124, CB	Arg^+	11	1.577	−3.020	9.631
50, CD1	Leu	4	5.430	0.997	6.596	125, C	Arg^+	11	2.719	−3.873	11.678
51, CD2	Leu	4	3.074	1.083	7.534	126, O	Arg^+	11	2.466	−3.348	12.761
52, HD1	Leu	4	5.925	0.914	7.564	127, HB	Arg^+	11	1.788	−3.142	8.569
53, HD1	Leu	4	6.042	0.517	5.833	128, HB	Arg^+	11	0.967	−3.870	9.935
54, HD1	Leu	4	5.296	2.049	6.346	129, CG	Arg^+	11	0.801	−1.721	9.856
55, HD2	Leu	4	3.391	2.124	7.608	130, HG	Arg^+	11	−0.223	−1.952	10.152
56, HD2	Leu	4	2.082	1.037	7.085	131, HG	Arg^+	11	1.251	−1.161	10.676
57, HD2	Leu	4	3.044	0.641	8.529	132, CD	Arg^+	11	0.790	−0.862	8.590
58, N	Ala	5	1.026	−1.592	4.184	133, HD	Arg^+	11	0.646	0.186	8.853
59, HN	Ala	5	1.211	−1.004	3.396	134, HD	Arg^+	11	1.753	−0.935	8.084
60, CA	Ala	5	−0.347	−2.055	4.294	135, NE	Arg^+	11	−0.292	−1.309	7.685
61, HA	Ala	5	−0.646	−1.960	5.338	136, HE	Arg^+	11	−0.192	−2.197	7.237
62, CB	Ala	5	−1.256	−1.169	3.439	137, CZ	Arg^+	11	−1.398	−0.597	7.427
63, C	Ala	5	−0.418	−3.528	3.887	138, NH2	Arg^+	11	−2.602	−1.092	7.745
64, O	Ala	5	−1.177	−4.301	4.470	139, NH1	Arg^+	11	−1.300	0.610	6.853
65, HB	Ala	5	−1.150	−0.131	3.754	140, HH1	Arg^+	11	−1.536	1.431	7.372
66, HB	Ala	5	−0.972	−1.262	2.391	141, HH1	Arg^+	11	−0.990	0.689	5.905
67, HB	Ala	5	−2.292	−1.483	3.565	142, HH2	Arg^+	11	−3.192	−1.468	7.030
68, N	Glu^-	6	0.382	−3.873	2.889	143, HH2	Arg^+	11	−2.910	−1.085	8.696
69, HN	Glu^-	6	0.997	−3.238	2.421	144, N	NH	12	2.866	−5.177	11.493
70, CA	Glu^-	6	0.420	−5.239	2.398	145, H	NH	12	3.073	−5.597	10.609
71, HA	Glu^-	6	−0.570	−5.423	1.978	146, C	CH_3	12	2.733	−6.110	12.599
72, CB	Glu^-	6	1.469	−5.397	1.295	147, H3	CH_3	12	3.476	−5.877	13.362
73, C	Glu^-	6	0.684	−6.211	3.549	148, H3	CH_3	12	1.734	−6.026	13.027
74, O	Glu^-	6	1.762	−6.198	4.142	149, H3	CH_3	12	2.890	−7.126	12.238
75, HB	Glu^-	6	2.453	−5.136	1.685						

and Gly(13) were found to assume backbone conformations in the region of positive values of ϕ in the ϕ–ψ map (Table II) (Zimmerman et al., 1977), although other types of conformations for Gly(14) were also compatible with the TRNOE distance constraints. This helps explain the observations that Gly(12) and Gly(13) are strongly conserved (Blombäck, 1967; Henschen et al., 1983) and that a single mutation of Gly(12) to Val(12) in fibrinogen produces bleeding disorders (Henschen et al., 1983; Ménaché, 1983). The Val substitution presumably disrupts the type II β-turn conformation involving residues Glu(11) and Gly(12), since a backbone conformation of Val in the region of positive values of ϕ in the ϕ–ψ map would have relatively high energy (Zimmerman et al., 1977) and a Val residue has been found, in most crystal structures of peptides and proteins, to assume negative values of ϕ in the ϕ–ψ map (Némethy & Scheraga, 1977; Richardson, 1981; Iijima et al., 1987). In a previous study, it was found that the inhibitory effects on thrombin action were very small for Bzl-peptide methyl esters with a Phe residue at other than the natural P9 position (residue 8) (Blombäck et al., 1969). The reduced inhibitory actions of these synthetic peptides were, however, found to be partially restored if there is a Phe residue at the P3 position [naturally Gly(14)]. Inspection of the structures in Figure 7 leads to a possible explanation for this interesting observation. If we assume that Phe(8) is directly in contact with thrombin, then residues Leu(9), Ala(10), and Glu(11) assume positions further away from the contact site. Furthermore, the aromatic side chain, when Phe is substituted at these positions, probably would not assume optimal orientation for binding to a complementary site at the active site of thrombin. Replacement of Gly(12) by Phe(12) would destabilize the type II β-turn at the P6 [Glu(11)] and P5 [Gly(12)] positions since the probability for a Phe residue to assume a backbone conformation in the region of positive values of ϕ in the ϕ–ψ map is rather small (Zimmerman et al., 1977; Némethy & Scheraga, 1977; Richardson, 1981; Iijima et al., 1987). Residues Gly(13) and Gly(14) are brought back toward the thrombin–peptide interface by the β-bend structure at Glu(11) and Gly(12). Thus, substitution of a Phe residue at position P4 would again increase the inhibitory effect of the corresponding peptide. When a Phe residue occupies the position of Gly(14) (P3), the inhibitory effect is partially restored, presumably because, in the native structure, the aromatic moiety of the side chain of Phe(8) lies between the C^{α} carbon of Phe(8) and the C^{α} carbon of Gly(14) (Figure 7), as indicated by the transferred NOEs between the meta and para protons of the aromatic ring of Phe(8) and the $C^{\alpha}H$ protons of Gly(14) (Figure 5B).

Conclusions

The interaction of bovine thrombin with the Arg–Gly binding site on the Aα chain of human fibrinogen has been studied by use of high-resolution NMR techniques. The specificity of the interaction was found to lie within the sequence of residues Asp(7)–Arg(16) (Ni et al., 1989). The thrombin-bound structure of a synthetic peptide corresponding to this specificity sequence was determined by a combination of transferred NOE measurements and distance geometry calculations. A predominant feature of the thrombin-recognized structure is the complementary hydrophobic combining site formed by the nonpolar side chains of Phe(8), Leu(9), and Val(15) within fibrinopeptide A (FpA) that is released upon the conversion of fibrinogen to fibrin. This hydrophobic binding site is brought about by an α-helical structure from residue Phe(8) to residue Ala(10), followed by a multiple-turn structure from residue Glu(11) to residue Val(15). Residue Asp(7) serves to stabilize these structural features through a hydrogen bond between its backbone carbonyl oxygen and the NH proton of Glu(11) and possibly also through a hydrogen bond between its side-chain carboxylate oxygens and the NH proton of Leu(9). Work is in progress on the effect of the Gly(12) to Val(12) substitution on the structure of the thrombin-bound peptide (Ni, Konishi, and Scheraga, unpublished results) and on the quantitative assessments of the contribution of each amino acid residue within residues Asp(7)–Val(20) to the specificity of the interaction of thrombin with fibrinogen (Ashton, Konishi, and Scheraga, unpublished results).

Acknowledgments

We thank T. W. Thannhauser and R. W. Sherwood of the Cornell University Biotechnology Program Facility for carrying out the amino acid analyses. Distance geometry computations were carried out on the Cornell National Supercomputer Facility, a resource of the Center for Theory and Simulation in Science and Engineering, which is funded in part by the National Science Foundation, New York State, and the IBM Corp. We thank Drs. Y. Konishi and S. T. Lord for comments on the manuscript and M. Adler and M. J. Dudek for helpful discussions. We also thank the staff members of the Syracuse NIH Regional Resource Facility for Multinuclear NMR and Data Processing, particularly G. Heffron and A. Lipton for maintaining the spectrometer and for their technical assistance. We gratefully acknowledge New Methods Research, Inc. (Syracuse) for providing the NMR1/NMR2 software system for the Sun workstation.

Registry No. F6, 74360-78-4; tF6, 118921-84-9; F8, 86177-72-2; tF8, 118949-41-0; thrombin, 9002-04-4.

References

Berliner, L. J. (1984) *Mol. Cell. Biochem. 61*, 159.

Berliner, L. J., Bauer, R. S., Chang, T. L., Fenton, J. W., II, & Shen, Y. Y. Lee (1981) *Biochemistry 20*, 1831.

Bidlingmeyer, B. A., Cohen, S. A., & Tarvin, T. L. (1984) *J. Chromatogr. 336*, 93.

Billeter, M., Braun, W., & Wüthrich, K. (1982) *J. Mol. Biol. 155*, 321.

Blombäck, B. (1967) in *Blood Clotting Enzymology* (Seegers, W. H., Ed.) pp 143–215, Academic Press, New York.

Blombäck, B., Blombäck, M., Olsson, P., Svendsen, L., & Aberg, G. (1969) *Scand. J. Clin. Lab. Invest., Suppl. 24(107)*, 59.

Braun, W., & Gō, N. (1985) *J. Mol. Biol. 186*, 611.

Claeson, G., Aurell, L., Karlsson, G., & Friberger, P. (1977) in *New Methods for the Analysis of Coagulation Using Chromogenic Substrates* (Witt, I., Ed.) p 37, de Gruyter, Berlin.

Clore, G. M., Brünger, A. T., Karplus, M., & Gronenborn, A. M. (1986) *J. Mol. Biol. 191*, 523.

Dwek, R. A. (1973) *Nuclear Magnetic Resonance in Biochemistry, Applications to Enzyme Systems*, Clarendon, Oxford, U.K.

Fesik, S. W., Bolis, G., Sham, H. L., & Olejniczak, E. T. (1987) *Biochemistry 26*, 1851.

Gerig, J. T., & Reinheimer, J. D. (1970) *J. Am. Chem. Soc. 92*, 3146.

Ghosh, A., & Seegers, W. H. (1980) *Thromb. Res. 20*, 281.

Henschen, A., Lottspeich, F., Kehl, M., & Southan, C. (1983) *Ann. N.Y. Acad. Sci. 408*, 28.

Iijima, H., Dunbar, J. B., Jr., & Marshall, G. R. (1987) *Proteins 2*, 330.

Kabsch, W., & Sander, C. (1983) *Biopolymers 22*, 2577.

Leach, S. J., Némethy, G., & Scheraga, H. A. (1977) *Biochem. Biophys. Res. Commun. 75*, 207.
Levitt, M., & Greer, J. (1977) *J. Mol. Biol. 114*, 181.
Lewis, P. N., Momany, F. A., & Scheraga, H. A. (1973) *Isr. J. Chem. 11*, 121.
Macura, S., & Ernst, R. R. (1980) *Mol. Phys. 41*, 95.
Marsh, H. C., Jr., Meinwald, Y. C., Lee, S., & Scheraga, H. A. (1982) *Biochemistry 21*, 6167.
Marsh, H. C., Jr., Meinwald, Y. C., Thannhauser, T. W., & Scheraga, H. A. (1983) *Biochemistry 22*, 4170.
Marsh, H. C., Jr., Meinwald, Y. C., Lee, S., Martinelli, R. A., & Scheraga, H. A. (1985) *Biochemistry 24*, 2806.
Meinwald, Y. C., Martinelli, R. A., van Nispen, J. W., & Scheraga, H. A. (1980) *Biochemistry 19*, 3820.
Ménaché, D. (1983) *Ann. N.Y. Acad. Sci. 408*, 121.
Momany, F. A., McGuire, R. F., Burgess, A. W., & Scheraga, H. A. (1975) *J. Phys. Chem. 79*, 2361.
Némethy, G., & Scheraga, H. A. (1977) *Q. Rev. Biophys. 10*, 239.
Ni, F., Scheraga, H. A., & Lord, S. T. (1988) *Biochemistry 27*, 4481.
Ni, F., Konishi, Y., Frazier, R. B., Scheraga, H. A., & Lord, S. T. (1989) *Biochemistry* (preceding paper in this issue).
Olejniczak, E. T., Gample, R. T., Jr., Rockway, T. W., & Fesik, S. W. (1988) *Biochemistry 27*, 7124.
Presta, L. G., & Rose, G. D. (1988) *Science 240*, 1632.
Rae, I. D., & Scheraga, H. A. (1979) *Int. J. Pept. Protein Res. 13*, 304.
Richardson, J. S. (1981) *Adv. Protein Chem. 34*, 167.
Richardson, J. S., & Richardson, D. C. (1988) *Science 240*, 1648.
Rose, G. D., Gierasch, L. M., & Smith, J. A. (1985) *Adv. Protein Chem. 37*, 1.
Solomon, I. (1955) *Phys. Rev. 99*, 559.
van Nispen, J. W., Hageman, T. C., & Scheraga, H. A. (1977) *Arch. Biochem. Biophys. 182*, 227.
Vásquez, M., & Scheraga, H. A. (1988) *J. Biomol. Struct. Dyn. 5*, 757.
Wagner, G., Neuhaus, D., Wörgötter, E., Vasak, M., Kagi, J. H. R., & Wüthrich, K. (1986) *J. Mol. Biol. 187*, 131.
Williamson, M. P., Havel, T. F., & Wüthrich, K. (1985) *J. Mol. Biol. 182*, 295.
Winzor, D. J., & Scheraga, H. A. (1964) *Arch. Biochem. Biophys. 104*, 202.
Wüthrich, K. (1986) *NMR of Proteins and Nucleic Acids*, Wiley, New York.
Wüthrich, K., Billeter, M., & Braun, W. (1983) *J. Mol. Biol. 169*, 949.
Wüthrich, K., Billeter, M., & Braun, W. (1984) *J. Mol. Biol. 180*, 715.
Zimmerman, S. S., Pottle, M. S., Némethy, G., & Scheraga, H. A. (1977) *Macromolecules 10*, 1.